Cell PRESS

Immunity

Article

The Heterodimeric Assembly of the CD94-NKG2 Receptor Family and Implications for Human Leukocyte Antigen-E Recognition

Lucy C. Sullivan,[1,4] Craig S. Clements,[2,4] Travis Beddoe,[2] Darryl Johnson,[1] Hilary L. Hoare,[2] Jie Lin,[1] Trevor Huyton,[2] Emma J. Hopkins,[2] Hugh H. Reid,[2] Matthew C.J. Wilce,[2] Juraj Kabat,[3] Francisco Borrego,[3] John E. Coligan,[3] Jamie Rossjohn,[2,5,*] and Andrew G. Brooks[1,5,*]

[1]Department of Microbiology and Immunology, University of Melbourne, Parkville, Victoria 3010, Australia

[2]The Protein Crystallography Unit, ARC Centre of Excellence in Structural and Functional Microbial Genomics, Department of Biochemistry and Molecular Biology, School of Biomedical Sciences, Monash University, Clayton, Victoria 3800, Australia

[3]Laboratory of Immunogenetics, National Institute of Allergy and Infectious Disease, National Institutes of Health, 12441 Parklawn Drive, Twinbrook II, Room 205, Rockville, MD 20852-1742, USA

[4]These authors contributed equally to this work.

[5]These authors contributed equally to this work.

*Correspondence: jamie.rossjohn@med.monash.edu.au (J.R.), agbrooks@unimelb.edu.au (A.G.B.)

DOI 10.1016/j.immuni.2007.10.013

SUMMARY

The CD94-NKG2 receptor family that regulates NK and T cells is unique among the lectin-like receptors encoded within the natural killer cell complex. The function of the CD94-NKG2 receptors is dictated by the pairing of the invariant CD94 polypeptide with specific NKG2 isoforms to form a family of functionally distinct heterodimeric receptors. However, the structural basis for this selective pairing and how they interact with their ligand, HLA-E, is unknown. We describe the 2.5 Å resolution crystal structure of CD94-NKG2A in which the mode of dimerization contrasts with that of other homodimeric NK receptors. Despite structural homology between the CD94 and NKG2A subunits, the dimer interface is asymmetric, thereby providing a structural basis for the preferred heterodimeric assembly. Structure-based sequence comparisons of other CD94-NKG2 family members, combined with extensive mutagenesis studies on HLA-E and CD94-NKG2A, allows a model of the interaction between CD94-NKG2A and HLA-E to be established, in which the invariant CD94 chain plays a more dominant role in interacting with HLA-E in comparison to the variable NKG2 chain.

INTRODUCTION

Natural killer (NK) cells play an important role in innate immune responses to viral infection (Lodoen and Lanier, 2005). Their activity is regulated in part through an array of activating and inhibitory receptors that recognize MHC class Ia, class Ib, and class I-like molecules. These receptors include the killer cell immunoglobulin-like receptors (KIR), immunoglobulin-like transcripts ILT (Cella et al., 2000), Ly49 receptors, and the more evolutionary conserved receptors of the C-type lectin (NKC) superfamily, including NKG2D and the CD94-NKG2 family (Borrego et al., 2006). However, in stark contrast to the CD69, NKG2D, and Ly49 family members, which are homodimeric receptors, CD94 is found as a heterodimer in vivo, paired with specific members of the NKG2 receptor family (Brooks et al., 1997; Carretero et al., 1997; Lazetic et al., 1996; Li et al., 2001; Natarajan et al., 2000; Tormo et al., 1999). Although a crystallographic CD94 homodimer has been observed, the structural basis for the preferred heterodimeric assembly of CD94-NKG2 receptors has remained unclear.

Because CD94 lacks cytoplasmic signaling motifs, the association of CD94 with NKG2 subunits is critical for the biological activity of this family. Several members of the NKG2 family including NKG2A, -2B, -2C, -2E, and -2H dimerize with CD94 in vitro (Brostjan et al., 2002; Kaiser et al., 2005; Lazetic et al., 1996). Moreover, there is evidence that alternate mRNA splicing may generate additional isoforms of both inhibitory and activating receptors (Houchins et al., 1997; Bellón et al., 1999). NKG2A (and its alternatively spliced variant NKG2B) contains cytoplasmic ITIM motifs that are typical of inhibitory receptors in other NK cell receptor families such as KIR (Houchins et al., 1991). In contrast, NKG2E or -2H and NKG2C contain a positively charged residue in their transmembrane region that facilitates their association with the ITAM-containing adaptor protein DAP-12 and hence appear to function as activating receptors (Lanier et al., 1998). However, as with KIR, the in vivo role of activating isoforms of NKG2 remains unclear.

Human CD94-NKG2A as well as other human CD94-NKG2 receptors recognize the class Ib molecule HLA-E (Borrego et al., 1998; Braud et al., 1998a; Brooks et al., 1999; Lee et al., 1998), whereas murine CD94-NKG2 receptors recognize the class Ib molecule Qa-1b (Vance

et al., 1998, 1999). The interaction of CD94-NKG2A with HLA-E is a central mechanism by which NK cells indirectly monitor the expression of other MHC class I molecules within a target cell. Because HLA-E has evolved to bind conserved sequences derived from their leader sequences of MHC-I, the optimal surface expression of HLA-E is dependent on the expression of other MHC class I molecules. In addition, because the loading of these peptides into HLA-E requires proteasomal trimming and a functional TAP, cell-surface expression of HLA-E may represent a surrogate marker for functional antigen processing necessary for the expression of other MHC class I molecules (Bland et al., 2003; Braud et al., 1998b).

Here we report the structure of the CD94-NKG2A heterodimer, which reveals the basis for the preferred formation of heterodimers within the CD94-NKG2 receptor family. Moreover, the structure of the CD94-NKG2A receptor, coupled with binding data assessing the interaction with HLA-E, has permitted a model for the CD94-NKG2A interaction with HLA-E to be proposed.

RESULTS

Expression, Purification, and Structure Determination

The extracellular region of CD94-NKG2A, which encompassed the C-type lectin domain and part of the N-terminal stalk region for each protomer (NKG2A, residues 100–233; CD94, residues 34–179), were expressed initially via a baculovirus expression system. However, limited proteolysis of the stalk regions, combined with glycosylation, resulted in a recombinant CD94-NKG2A receptor that, although interacting with HLA-E with similar affinity to that previously reported (data not shown) (Kaiser et al., 2005; Vales-Gomez et al., 1999), was too heterogeneous for structural studies. Consequently, the ectodomains of CD94 and NKG2A, spanning residues 40–179 and 110–233, respectively, were expressed in *Eschericia coli* and subsequently refolded and purified to homogeneity. The *E. coli*-derived CD94-NKG2A ectodomain interacted with HLA-E with identical affinity to that of the baculovirus-derived CD94-NKG2A, indicating that glycosylation of CD94-NKG2A is not required for ligand recognition (data not shown). Moreover, reduced and nonreduced SDS-PAGE analysis revealed that the baculovirus- and *E. coli*-derived CD94-NKG2A behaved in a very similar manner, which included evidence for the presence of an intermolecular disulfide bond. Collectively, this indicated that the refolded CD94-NKG2A receptor is a bona fide representative of the CD94-NKG2A receptor found on the cell surface. The refolded CD94-NKG2A receptor crystallized in space group $P2_1$, with unit cell dimensions a = 44.7 Å, b = 34.7 Å, c = 152.9 Å, β = 89.7°, with two heterodimers in the asymmetric unit (Table 1). The structure was subsequently refined to 2.5 Å resolution, to an R_{fac} and R_{free} of 23.4% and 27.0%, respectively. The final model comprises amino acids 57–179 of CD94 and 113–232 of NKG2A, together with 51 water molecules (for clarity, NKG2A and CD94 numbering has the suffixes A and B, respectively). The two molecules in the asymmetric unit are virtually identical (root mean square deviation [rmsd] 0.05 Å), and structural analyses will be confined to one molecule of the asymmetric unit. The electron density at the dimer interface and the region corresponding to the HLA-E binding site, with the exception of one small disordered region (residues 200A to 203A), was unambiguous, thereby permitting the salient features of the CD94-NKG2A heterodimer to be analyzed.

Table 1. Data Collection and Refinement Statistics

Data Collection Statistics	
Temperature (K)	100
X-ray source	IMCA, APS
Detector	Quantum 210 CCD
Space group	$P2_1$
Cell dimensions (Å)	44.7, 34.7, 152.9
Cell angles (°)	90, 89.7, 90
Resolution (Å)	76.5-2.5 (2.64-2.5)
Total no. of observations	52,441 (6,039)
No. of unique observations	16,457 (2,242)
Multiplicity	3.2 (2.7)
Data completeness (%)	98.5 (93.6)
I/σ_I	10.1 (2.2)
R_{sym} [a] (%)	12.2 (21.9)
Refinement Statistics	
Nonhydrogen atoms	
Protein	3871
Water	51
Resolution (Å)	2.5
R_{factor} [b] (%)	23.4
R_{free} [b] (%)	27.0
Rmsd from ideality	
Bond lengths (Å)	0.009
Bond angles (°)	1.234
Ramachandran plot	
Most favored (%)	85.6
Allowed regions (%)	14.4
B factors (Å^2)	
Average protein	41.1
Average water molecule	46.7

The values in parentheses are for the highest resolution bin (approximate interval 0.1 Å).
[a] $R_{sym} = 100 \cdot \Sigma\, |I_{hkl} - < I_{hkl} > |/\Sigma I_{hkl}$.
[b] $R_{factor} = 100 \cdot \Sigma_{hkl}\, ||F_o| - |F_c||/\Sigma_{hkl}\, |F_o|$ for all data except for 5%, which was used for the R_{free} calculation.

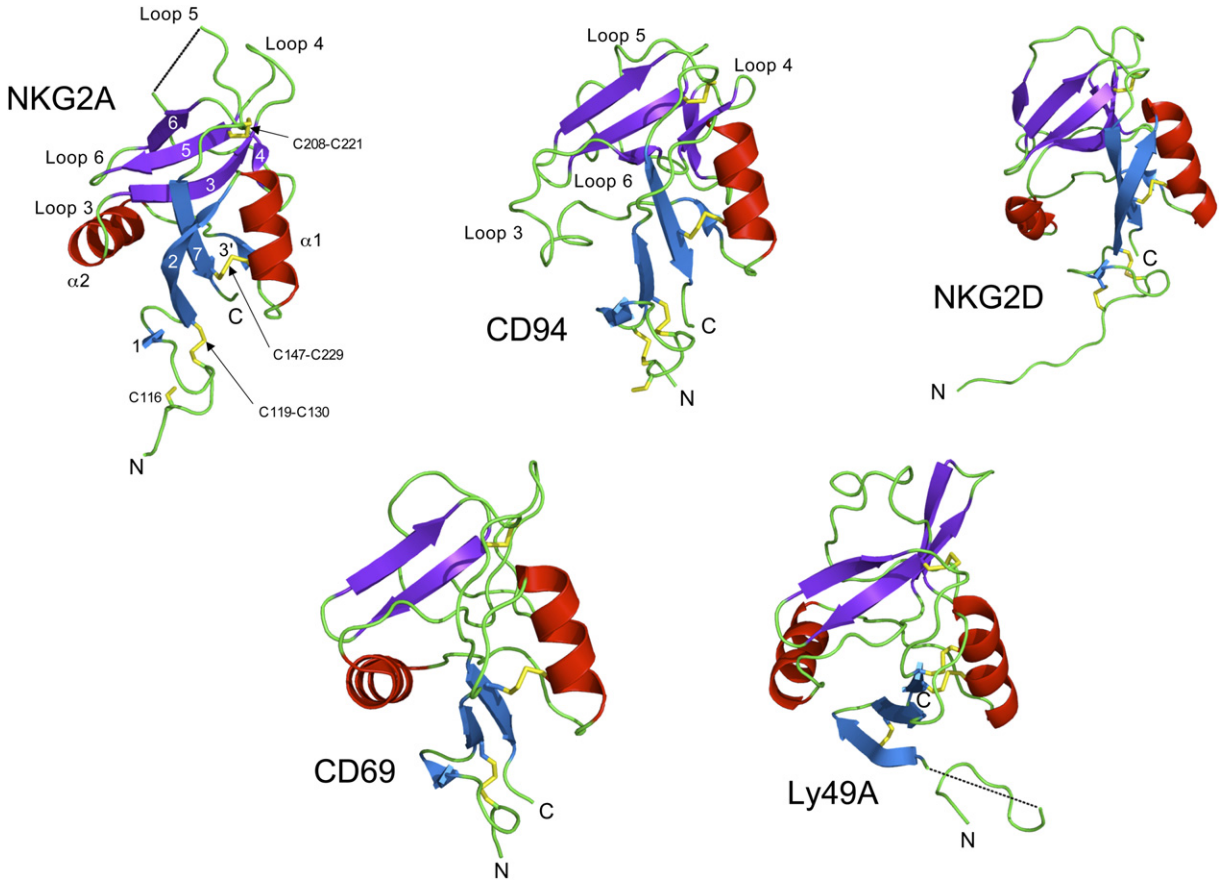

Figure 1. NKG2A and the C-type Lectin Family

NKG2A has a C-type lectin fold as seen in NKG2D (Protein Data Bank ID code 1MPU), CD94 (1B6E), CD69 (1E8I), and Ly49A (1QO3). The β strands are shown in blue and purple, the α helices in red, and disulfide bonds are in yellow. The secondary structure elements are labeled according to the CD94 nomenclature (Boyington et al., 1999).

The NKG2A Subunit

The NKG2A monomer (Figure 1) possesses a meandering N-terminal region (residues 113–118) that connects the core of the molecule to the membrane-proximal stalk region. The NKG2A ectodomain, with overall dimensions ~54 × 33 × 29 Å, comprises eight β strands that form two β sheets at approximate right angles to each other, and two α helices (residues 140–149 and 160–169) on opposing faces of the protomer. The NKG2A fold is stabilized by three disulfide bonds: Cys119–Cys130, bridging the N-terminal loop and the β2 strand; Cys147–Cys229, bridging α1 helix and β7 strand; and Cys208–Cys221, that connects the β5 strand to loop 6.

As expected, the NKG2A fold is structurally homologous to the C-type lectins, and the comparative structural analyses will be confined to the NKC receptor family, namely CD94 (this study and Boyington et al., 1999), NKG2D (Li et al., 2001, 2002; McFarland et al., 2003; Wolan et al., 2001), CD69 (Natarajan et al., 2000), and Ly49 (Tormo et al., 1999). NKG2A is most structurally related to CD94 (91 Cα atoms, rmsd 1.13 Å, 28% sequence identity), followed by murine NKG2D (97 Cα atoms, rmsd 1.27 Å, 26.7% sequence identity); Ly49A (93 Cα atoms, rmsd 1.29 Å, 28.9% sequence identity); human NKG2D (95 Cα atoms, rmsd 1.44 Å, 22.4% sequence identity); and CD69 (94 Cα atoms, rmsd 1.74 Å, 26.7% sequence identity). The structural comparisons reveal that despite the low sequence identity, the overall fold, which includes the two β sheets, the α1 helix, and the positioning of the three canonical C-type lectin disulfide bonds, is well conserved. The largest area of structural divergence between NKG2A and the other NKC receptors lies at the dimerization site, which includes the N-terminal region, as well as the presence or orientation of the α2 helix, and the loops that are implicated in ligand recognition (Figure 1). For example, in comparing the structures of NKG2A and CD94, the major structural differences correspond to the α2 helix and loop 3 (residues 160A–171A), which is replaced by a long and extended loop in CD94 (residues 97B–114B); loop 4 (residues 179A–186A), which points toward loop 5 (186A–207A) in NKG2A and away from loop 5 in CD94; and loop 5 itself, which, although long and flexible in both NKG2A and CD94, is structurally dissimilar (Figure 1). Accordingly, the NKG2A fold resembles CD94 and other

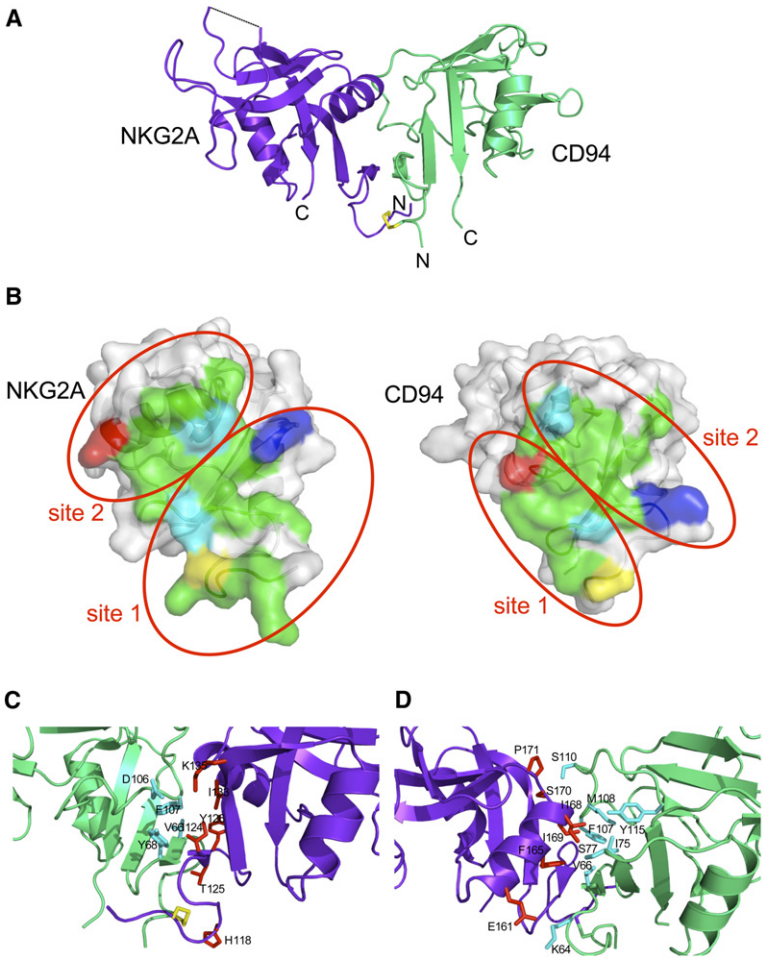

Figure 2. The CD94-NKG2A Heterodimer

(A) Ribbon representation of the overall structure of the heterodimer with NKG2A shown in purple, CD94 in green, and the interchain disulfide in yellow.

(B) Surface representation of the dimer interface highlighting the extensive interactions between the two subunits. Residues forming hydrogen bonds are shown in cyan, salt bridge partners are shown in red and blue, the cysteines that form the interchain disulfide are colored yellow, and residues involved in hydrophobic contacts are colored green.

(C and D) The two sites of interaction are labeled and shown in detail in (C) site 1 and (D) site 2. In these views, NKG2A residues involved in contacts are colored red and the corresponding CD94 residues are shown in cyan.

NKC receptors, with the largest structural differences residing in areas that interact with ligand and the dimerization interface (Figures 1 and 2).

Heterodimeric Assembly

NKG2A, and closely related members of the NKG2 family, form obligate heterodimers with CD94 on the cell surface, whereas structurally related NKC-encoded receptors such as NKG2D, NKR-P1, CD69, and the Ly49 receptors are all cotranslationally assembled as homodimers (Sawicki et al., 2001). Accordingly, the CD94-NKG2A structure provides insight into the specificity of heterodimer formation within the CD94-NKG2 family. CD94-NKG2A forms an elongated dimer, with dimensions 75 × 42 × 38 Å, and the two subunits are related by an almost perfect 2-fold (175°) (Figure 2). The dimer interface is large, comprising approximately 1500 $Å^2$ of buried surface area (BSA). The interface shows good shape complementarity (SC index = 0.6) and is dominated by nonpolar interactions that comprise ~2/3 of the interface (Figure 2B; Table S1 available online). The hydrophobic interactions are centrally located, whereas the two salt bridges (Glu161A and Lys135A salt-bridged to Lys64B and Asp106B, respectively) are on the periphery of the interface (Figures 2C and 2D). The mode of CD94-NKG2A dimerization includes main chain H-bonding between the respective β1 strands, creating an extended 6-stranded antiparallel β sheet at the core of the dimer interface (Figure 2). The CD94-NKG2A interface shares some features with the NKC homodimers, including a large buried surface area (ranging from 1220 $Å^2$ in CD94 to 2800 $Å^2$ in human NKG2D) that exhibits high shape complementarity, the extended central β sheet, and a large number of hydrophobic contacts. Nevertheless, the relative juxtapositioning of the subunits between the homodimeric NKC receptors and CD94-NKG2A dimers was variable; for example, although the CD69 dimer (Natarajan et al., 2000) was the most similar (0.3°), the Ly49A homodimer (Tormo et al., 1999) deviated by 36.5° when compared to CD94-NKG2A (Figure S1).

Despite the structural homology between NKG2A and CD94, the dimer interface is asymmetric, as a result of structural differences between these subunits residing at the interface. Accordingly, the mode of CD94-NKG2A dimerization is distinct from the symmetric homodimeric NK receptors. There are two distinct stretches of primary structure within NKG2A, which we term site 1 and site 2, that participate in mediating contacts at the dimer interface, and these sites form a continuous interaction surface

within the heterodimer. Site 1, which spans residues 114A–135A, includes the N-terminal region that extends toward the corresponding region in CD94 (residues 58B–70B). This cysteine-rich region of the dimer contains the intermolecular disulfide bond (Cys116A to Cys59B), which is consistent with the observation of an intermolecular disulfide bond via SDS-PAGE analysis. Cys116A is shielded largely from solvent, whereas Cys59B is more solvent accessible, yet partly occluded. Centered on the β1 strand pairing is a small hydrophobic cluster that includes Val66B and Tyr68B and Ile124A and Tyr126A. This hydrophobic cluster merges into site 2, where residues (spanning residues 165A to 170A) located at the C-terminal region of the α2 helix of NKG2A play a central role interacting with residues 107B–110B from CD94. Phe165A interacts with Val66B; Ile168A interacts with side chains of Ile75B, Ser77B, and Tyr115B; Ile169A interacts with Phe107B and Met108B; and Ser170A and Pro171A interact with Ser110B. Although the site 1 interaction is relatively well conserved between CD94-NKG2A and the homodimeric NKC receptors, site 2 differs with the α2 helix that interacts with the long and extended loop in CD94, varying in length and orientation in comparison to other NKC receptors. In summary, the data indicate that asymmetric interactions drive the heterodimeric assembly of the receptor.

The NKG2 Receptor Family

The NKG2 receptor family comprises NKG2A, -2B, -2C, -2D, -2E, -2F, and -2H. Of these, only NKG2D and NKG2F are incapable of pairing with CD94 in vitro. NKG2D functions as a homodimer and shares little sequence homology with the other NKG2 family members (McFarland et al., 2003; McFarland and Strong, 2003; Wu et al., 1999). NKG2F has a truncated ectodomain relative to the other members of this family and, although it can associate with DAP12, the function of this isoform currently remains unknown (Kim et al., 2004). The remaining members of this family, NKG2C, NKG2E, and NKG2H, exhibit high sequence identity with NKG2A in the C-type lectin domain (92% and 80%, respectively), suggesting a common mode of assembly with CD94. Consistent with this, 15 of the 18 dimerization contacts are conserved across NKG2A, NKG2B, NKG2C, and NKG2E (Figure 3).

Despite the high sequence identity between CD94-NKG2A and CD94-NKG2C, there is an approximate 6-fold difference in the affinity for HLA-E (Kaiser et al., 2005; Vales-Gomez et al., 1999). To understand the structural basis for this affinity differential, the amino acids that differ between NKG2A and NKG2C were mapped onto the structure of CD94-NKG2A. Two of these amino acids map to the putative HLA-E binding site, position 197 in loop 5 (Glu in NKG2A, Lys in NKG2C) and position 225 within loop 7 (Ile in NKG2A, Met in NKG2C). In addition, a cluster of different amino acids reside at the top of the molecule at the CD94-NKG2A interface (Ser167, Ile168, Ile169, and Ser170 in NKG2A compared with Ala165, Ser166, Ile167, and Leu168 in NKG2C; Figure 3B). Thus, the positioning of residues that differ between NKG2A and NKG2C in the heterodimer interface raises the possibility that the differences between CD94-NKG2A and CD94-NKG2C in their affinity for HLA-E may result from indirect effects of the NKG2 subunit on the conformation of CD94.

Substitutions to P8 Impact on the Affinity of CD94-NKG2A for HLA-E

The interaction of CD94-NKG2 receptors with HLA-E bound to the leader sequence peptides derived from MHC class I (residues 3–11) is sensitive to changes in the C-terminal region of the peptide and in particular P8 (Kaiser et al., 2005; Miller et al., 2003; Vales-Gomez et al., 1999). However, previous studies have largely been confined to the substitution of a small number of hydrophobic residues that are naturally found at this position in the leader sequences of class I molecules (residue 10 of MHC-I). Hence, the tolerance of the CD94-NKG2A receptor for less conservative substitutions at position P8 remains unknown. Consequently, we systematically made substitutions at this position, refolded these peptides with HLA-E, and then assessed their impact on the affinity for CD94-NKG2A by surface plasmon resonance (SPR; Table S2, Figure S2). By using this approach, we considered that less than a 3-fold change in affinity was insignificant, a 3- to 8-fold indicated a moderate effect, and >8-fold indicated a significant effect on the interaction.

Consistent with previous findings, HLA-E complexed to the peptide corresponding to the leader sequence peptide derived from HLA-G-bound CD94-NKG2A with an affinity of 0.94 μM (Kaiser et al., 2005; Vales-Gomez et al., 1999). The kinetics of the interaction were too rapid to allow accurate determination of the kinetic rate constants. Although this peptide has a Phe at P8, the amino acids present in this position of other class Ia-encoded leader sequence peptides are predominantly the hydrophobic residues Ile, Leu, or Val. Substitution of P8-Phe for each of these smaller hydrophobic residues decreased the affinity of HLA-E for CD94-NKG2A (Table S2). Specifically, the complexes with P8-Leu and P8-Val peptides bound with a 90% reduction in affinity; the P8-Ile substitution had a modest effect (2.97 μM); whereas the P8-Ala substitution, a residue not typically present in class I leader sequences, resulted in a 97% decrease in affinity. Similarly substitution with either Tyr or Lys at P8 (neither of which are present in the leader sequences of MHC-I) also reduced the affinity of the interaction to 19 μM and 34 μM, respectively, which indicated that polar and charged residues are not tolerated at position P8. In summary, the data suggests that there is a preference for a bulky, solvent-exposed hydrophobic residue at this position for optimal interaction with CD94-NKG2A.

Alanine Scanning Mutagenesis of HLA-E

The interaction with the CD94-NKG2 receptors was unlikely to be solely mediated by peptide contacts, so we made 16 individual alanine-scanning mutations in HLA-E that were subsequently refolded with the VMAPRTLFL peptide and assessed their ability to interact with CD94-NKG2A (Table 2). With the exception of the Lys146 mutant that failed to refold, all mutants refolded with similar yields

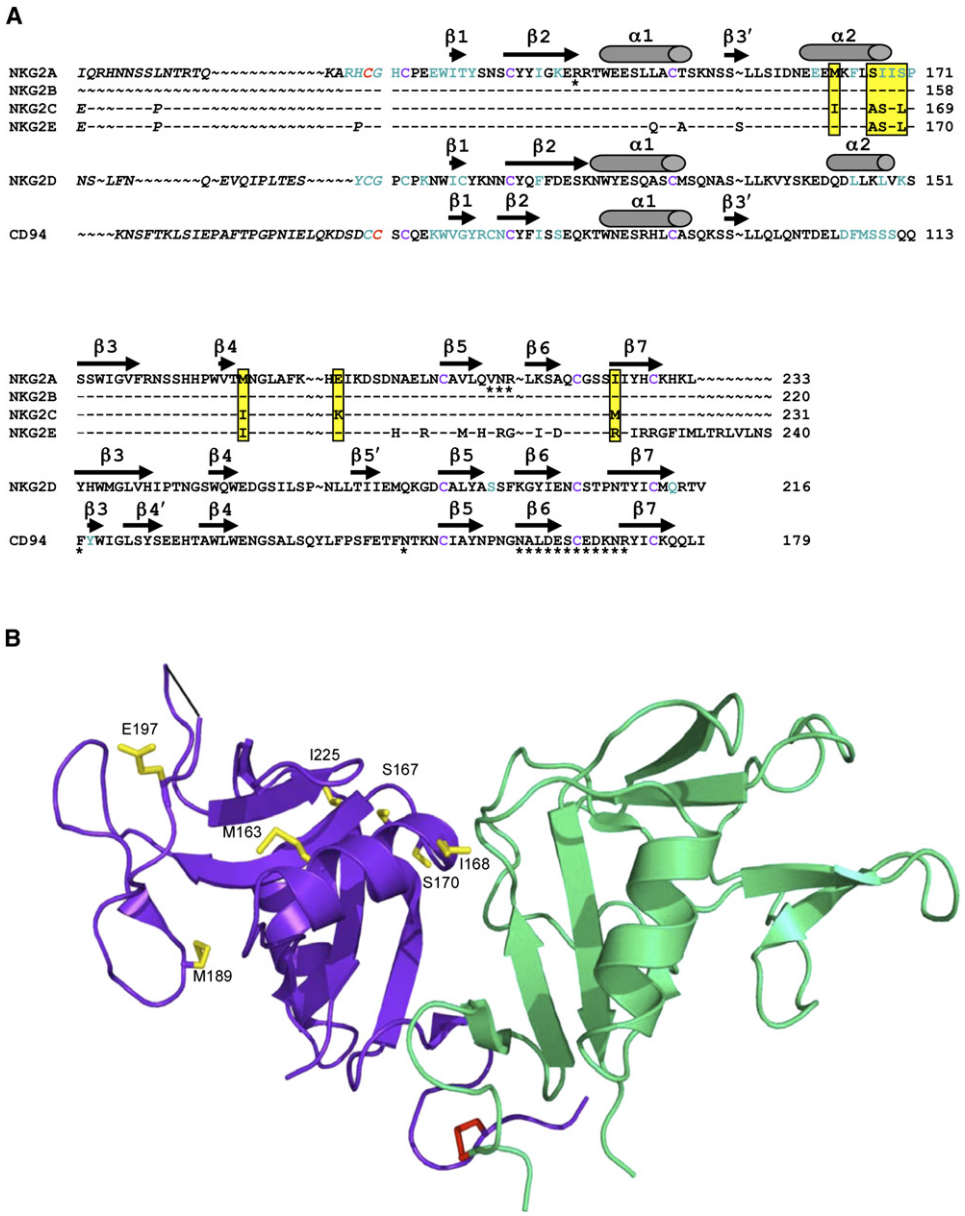

Figure 3. The NKG2x Family

(A) Sequence alignment of NKG2A with other NKG2 receptors and CD94. Sequence alignments of the stem (italics) and CTLD ectodomains of NKG2x and CD94, showing intrachain cysteines in purple. Residues conserved between NKG2A, -2B, -2C, -2E, and -2H are indicated by the dashes. Substitutions between NKG2A and -2C isoforms that could account for the difference in affinity for HLA-E are highlighted in yellow. Secondary structures for NKG2A, NKG2D, and CD94 are shown above the sequences, with cylinders representing α helices and arrows representing β sheets. Residues involved in homodimerization (NKG2D) or heterodimerization (NKG2A and CD94) are shown in cyan, with interchain cysteines colored in red. Asterisks indicate putative HLA-E binding sites on CD94 and NKG2A.

(B) Ribbon representation of CD94-NKG2A heterodimer with the residues that differ between NKG2A and NKG2C shown in yellow and the interchain disulfide bond shown in red.

to wild-type HLA-E. As expected, the Thr214 mutation in the α3 domain of HLA-E had no marked effect on the affinity of the interaction with CD94-NKG2A (Table 2). Substitution of many of the exposed charged residues (Arg62, Asp69, Glu89, Arg108, Asp149, and Glu154) in both the α1 and α2 helices of HLA-E also had little effect on its affinity for CD94-NKG2A (Figure 4). Similarly, mutation of His155, which makes contact with P5-Arg, had little effect on the affinity of HLA-E for CD94-NKG2A. However, mutation of Arg65, Arg79, and Glu166 had a modest impact on the affinity of the interaction. In contrast, mutation of Arg75 and Val76 that are proximal to P8-Phe had a substantial effect on the interaction with the Val76 mutation resulting in a 90% decrease in the affinity of the

Table 2. Affinity of Mutant HLA-E-Peptide Complexes for CD94-NKG2A

HLA-E Mutant	K_D (μM) CD94-NKG2A
Wild-type	0.94 ± 0.11
R62A	1.75 ± 0.45
R65A	3.05 ± 0.29
D69A	1.85 ± 0.84
Q72A	17.9 ± 4.05
R75A	>207
V76A	9.22 ± 0.78
R79A	5.23 ± 0.78
E89A	1.02 ± 0.45
R108A	1.69 ± 0.12
D149A	1.45 ± 0.13
E152A	23.13 ± 2.16
E154A	2.12 ± 0.12
H155A	1.76 ± 0.14
D162A	12.87 ± 2.20
E166A	3.08 ± 0.23
T214A	1.44 ± 0.06

Data are represented as means ± standard error of 2–5 experiments with independent preparations of refolded proteins.

interaction, and the Arg75 mutation essentially abrogated binding altogether (Table 2, Figure 4A). Mutation to Ala of either Gln72 or Glu152 that flank the P5-Arg also had a marked impact on recognition by CD94-NKG2A resulting in dissociation constants of 17.9 μM and 23.1 μM, respectively. Mutation of Asp162, a residue that is located on the α2 helix but does not make peptide contacts, decreased the affinity for CD94-NKG2A to 12.9 μM. Collectively, the mutagenesis data revealed that residues from both the α1 and α2 helices are critical for recognition, although the data were consistent with the α1 helix playing a more prominent role in the interaction than the α2 helix of HLA-E.

Alanine Scanning Mutagenesis of CD94-NKG2A

Although mutagenesis of HLA-E provided insight into the likely diagonal-mode of docking of the CD94-NKG2A receptor on HLA-E, the orientation of the CD94-NKG2A with respect to HLA-E was ambiguous; moreover, the relative contributions of the CD94 and NKG2A subunits to the interaction with HLA-E was unclear. To address these issues, a mutagenesis approach was again employed in which exposed residues on either CD94 or NKG2A were mutated to Ala and the affinity of the interaction between mutant receptor and HLA-E determined. In total, 21 CD94-NKG2A mutants were made, all of which refolded with an efficiency comparable to that of the wild-type receptor. Although mutation of CD94 residues Gln79B, Thr146B, Asn148B, and Asn158B had no substantial impact on the binding of CD94-NKG2A to HLA-E, a number of other mutations markedly reduced the affinity of the interaction (Table 3, Figure 4B). Notably, mutation of CD94 residues Gln112B and Phe114B, which are located at the C-terminal end of loop 3, abrogated binding to HLA-E. Similarly, mutation of either Asn160B or Leu162B, which are located at the C terminus of loop 6 and the beginning of the β6 strand, respectively, also abolished recognition of HLA-E. Moreover, the observation that mutation of the adjacent residues Asp163B and Glu164B also resulted in a greater than 90% reduction in affinity further suggested an important role for the β6 strand of CD94 in the interaction with HLA-E.

In contrast, no mutations of the NKG2A subunit resulted in a dramatic change in the affinity of the receptor for HLA-E (Table 3). Specifically, of the 10 mutants generated, none resulted in a 5-fold or greater decrease in the affinity of CD94-NKG2A for HLA-E, and only changes in Arg137A located in the β2 strand and Gln212A and Arg215A located at the end of the β5 strand and the adjacent loop resulted in modest decreases in the affinity of the interaction (Figure 4B). Thus, the CD94-NKG2A mutagenesis data demonstrate that CD94 plays a crucial role in providing energetically critical contacts whereas the role of NKG2A appears to be more limited.

A Model of the CD94-NKG2A Interaction with HLA-E

Based on the mutagenesis data and the structures of the nonliganded CD94-NKG2A receptor and the HLA-E molecules, we constructed a model of the ternary CD94-NKG2A-HLA-E complex, with the NKG2D-NKG2D ligand complexes as a template that is broadly consistent with earlier models that utilized the crystallographic dimer of CD94 and the NKG2D-MICA structure (Figure 4C). Our model suggests that the CD94-NKG2A docks in a mode that is diagonal to the long axis of the HLA-E Ag-binding cleft, such that the CD94 subunit is positioned mostly over the α1 helix and NKG2A over the α2 helix. This orientation is based on the observations that the majority of residues in HLA-E that are critical for the interaction are in the α1 helix flanking P5 and P8 and that there is "hotspot" in CD94 comprised of residues 112 and 114 together with 160 and 162–164 (Figure 4B). Thus, CD94 is predicted to mediate the contacts with the peptide, in agreement with the observation that substitutions at the C terminus of the peptide affect the interaction of all CD94-NKG2 receptors with HLA-E in a similar manner (Kaiser et al., 2005). This is also consistent with structural analyses by Li et al. (2001) and Kaiser et al. (2005) and the mutagenesis data from Wada et al. (2004). Indeed, consistent with our mutagenesis data, these studies identified a hydrophobic patch on HLA-E comprised of Ile73, Val76, and the side chain of P8, which was proposed to interact with a hydrophobic region on CD94 (Phe114, Leu162).

Further insight into the mode of CD94-NKG2-HLA-E recognition is provided by the observation that there is a 6-fold difference in affinity in the interaction between CD94-NKG2A and CD94-NKG2C (Kaiser et al., 2005;

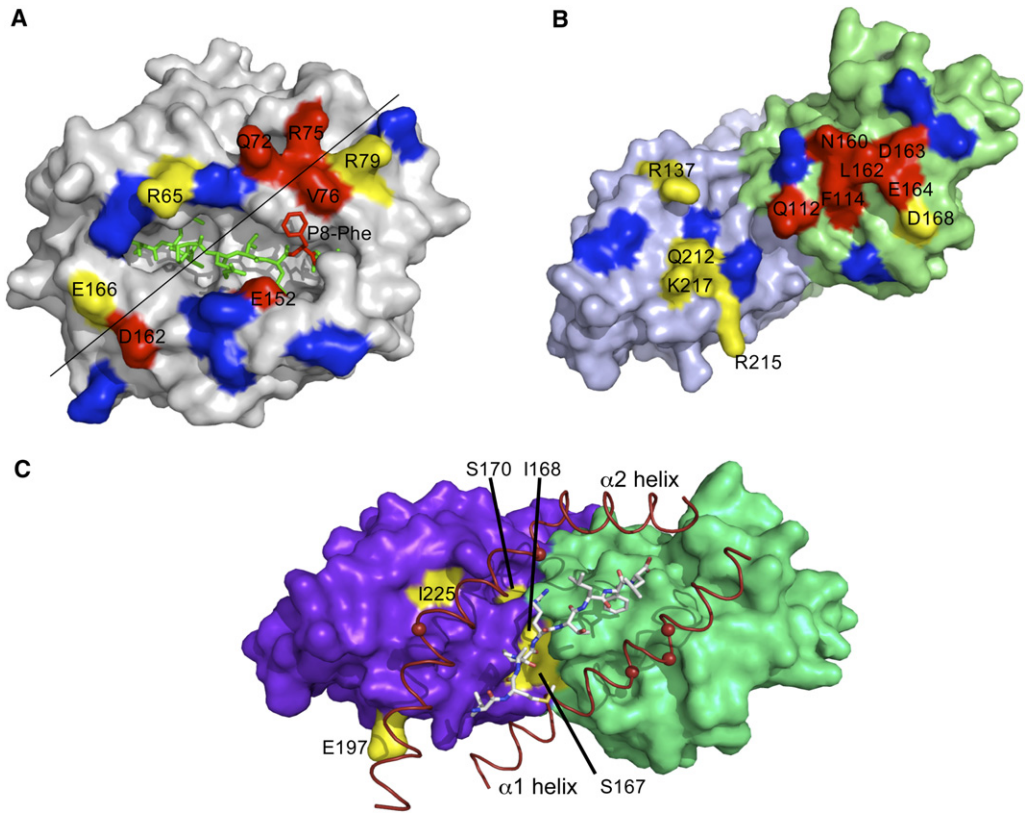

Figure 4. Recognition of HLA-E by CD94-NKG2A

(A and B) Individual HLA-E (A) and CD94-NKG2A (B) residues were mutated, and the affinity of the interaction between the proteins was measured by surface plasmon resonance. Residues that had a major influence on binding when mutated are shown in red, residues with a minor influence are in yellow, and residues that did not alter affinity for binding when mutated are shown in blue. The positioning of the residues that had the largest effect on binding affinity suggests a diagonal docking mode of CD94-NKG2A onto HLA-E (black line). CD94 and NKG2A subunits are colored light green and light blue, respectively.

(C) Model of CD94-NKG2A recognition of HLA-E. CD94-NKG2A docking on HLA-E-VMAPRTLFL was modeled on the NKG2D-MIC-A structure (1HYR). A surface representation of CD94-NKG2A is shown in purple (NKG2A) and green (CD94), with the α helices of HLA-E in red and the VMAPRTLFL peptide in white. Residues that differ between NKG2A and NKG2C are colored yellow. CD94-NKG2A binding hotspots on HLA-E, as identified by mutagenesis, are shown as red spheres.

Vales-Gomez et al., 1999). Of the sequence differences between NKG2A and NKG2C that are located within our candidate-docking site, position 197 was shown not to be a critical residue, because mutation of Glu197 of NKG2A to Lys that is present in NKG2C had little impact on affinity for HLA-E (Kaiser et al., 2005). Our crystallographic data suggest that the cluster of amino acid variability between NKG2A and NKG2C at the C-terminal end of the α2 helix of the NKG2 subunit was likely to play a key role, either directly by contacting HLA-E, or indirectly, by altering the conformation of the neighboring surface-exposed CD94 loop that, in accord with our model, interacts with the HLA-E. Consequently, to more formally address the impact of these differences on recognition of HLA-E, mutant CD94-NKG2A molecules were generated in which residues 167–170 in NKG2A (Ser-Ile-Ile-Ser) were replaced with those in NKG2C (Ala-Ser-Ile-Leu) (see Figure 3) or where residue 163, a Met in NKG2A, was exchanged for an Ile that is present at this position in NKG2C. Although the Met163Ile mutation had little impact on the interaction with HLA-E, the presence of the NKG2C sequences in the α2 helix of NKG2A decreased the affinity of the interaction with HLA-E by 83% (Table 3). To confirm that substitutions in the α2 helix of NKG2A were responsible for the differences in the affinity for CD94-NKG2A and -NKG2C for HLA-E, we replaced residues 161 and residues 165–168 with the corresponding amino acids from NKG2A. Consistent with the previous data, the Ile161Met mutation did not markedly impact on the interaction between CD94-NKG2C and HLA-E. However, replacement of NKG2C residues 165–168 (Ala-Ser-Ile-Leu) with the corresponding residues in NKG2A (Ser-Ile-Ile-Ser) resulted in an increase in the affinity of the interaction to 1.31 μM, a value similar to that observed for the HLA-E-CD94-NKG2A interaction. Together, these data not only provide insight into the interactions responsible for the different affinities of CD94-NKG2A and -NKG2C for HLA-E but also provide further support for the model of the interaction between CD94-NKG2 receptors and HLA-E.

Table 3. Affinity of Mutant CD94-NKG2A Complexes for HLA-E

Mutant	K_D (μM)
Wild-type	1.23 ± 0.12
CD94 Mutant	
Q79A	1.02 ± 0.09
Q112A	NB
F114A	NB
T146A	1.23 ± 0.07
N148A	0.77 ± 0.07
N158A	0.38 ± 0.04
N160A	NB
L162A	NB
D163A	17.24 ± 0.85
E164A	13.22 ± 0.84
D168A	4.76 ± 0.44
NKG2A Mutant	
R137A	4.13 ± 0.23
S172A	1.84 ± 0.16
D200A	0.79 ± 0.12
D202A	1.39 ± 0.12
Q212A	3.83 ± 0.46
V213A	1.95 ± 0.13
R215A	4.32 ± 0.29
K217A	3.12 ± 0.17
Q220A	2.88 ± 0.44
S223A	1.46 ± 0.09
Mutant	
NKG2C wt	6.88 ± 0.46
NKG2C I161M	6.62 ± 0.79
NKG2C 165-168SIIS	1.31 ± 0.18
NKG2A wt	1.54 ± 0.12
NKG2A M163I	1.46 ± 0.13
NKG2A 167-170ASIL	8.92 ± 0.85

Data are represented as means ± standard error of 2–5 experiments with independent preparations of refolded proteins.
NB: The interaction was too weak to allow an estimation of the K_D based on the concentration range of analyte.

DISCUSSION

Proteins with a C-type lectin fold play a prominent role in innate immunity, with soluble members providing innate defenses in mucosal fluids, whereas membrane-bound C-type lectins, such as the NKC receptor family, play a central role in the elimination of tumor and virus-infected cells (Kogelberg and Feizi, 2001). The NKC receptors are often found as homodimers as a result of homotypic interactions within the C-type lectin domain as well as interactions with the membrane-proximal regions of the receptors. However, the CD94-NKG2 family is atypical, preferentially forming heterodimeric receptors. This allows for a degree of biological adaptability such that a single ligand can induce either activating or inhibitory signals depending on the particular NKG2 subunit associated with CD94 and/or the relative levels of expression of the various NKG2 isoforms (Brooks et al., 1997; Carretero et al., 1997; Lazetic et al., 1996).

Although CD94 has the potential to form homodimers (Boyington et al., 1999), they exhibit poor shape complementarity and a low BSA at the dimer interface and their functional significance remains unclear. In contrast, we have observed no evidence of soluble NKG2A homodimers in in vitro refolding experiments (unpublished observations), and our attempts to generate an NKG2A homodimer in silico based on the CD94-NKG2A structure resulted in steric clashes with the α2 helix, which also would likely preclude the formation of the intermolecular disulfide bond. The data suggest that heterodimer formation is largely driven by interactions within the respective C-type lectin domains, which is evident in the extensive hydrophobic interface between these domains. Consistent with this, Lieto et al. (2006) identified an alternatively spliced form of CD94 that lacks 21 amino acids from the stem region that preferentially pairs with NKG2B (which itself is an alternatively spliced form of NKG2A that lacks 18 amino acids in the stem region) (Lieto et al., 2006). Collectively, this suggests that although the stalk regions of the CD94 and NKG2 subunits may contribute to the formation of the heterodimeric receptor, the driving forces for the assembly of CD94-NKG2 heterodimers are likely to be the innate attraction of the CD94 and NKG2 C-type lectin domains.

Given that NKG2A is structurally homologous to CD94 and other NKC receptors, a priori it was unclear why it would preferentially pair with CD94. The structure of the CD94-NKG2A heterodimer reveals that the mode of dimerization is driven not only via an intermolecular disulfide bond but also by asymmetric interactions. The asymmetry at the CD94-NKG2A interface is largely a result of the α2 helix of NKG2A interacting with the corresponding extended loop region of CD94. The high sequence identity among the NKG2 isoforms, as well as interspecies conservation, suggests that this mode of heterodimerization is conserved across the CD94-NKG2 family.

CD94-NKG2A is highly specific for HLA-E in complex with peptides derived from the leader sequence of MHC class I molecules (Borrego et al., 1998; Brooks et al., 1999; Llano et al., 1998; Vales-Gomez et al., 1999). The data here highlight the importance of P8 side chain for recognition of HLA-E by CD94-NKG2A. The observation that HLA-E bound to peptides with Ala, Tyr, or Lys at P8 interacts with CD94-NKG2A with low affinity suggests a role for this residue in governing the specificity of the interaction. Moreover, a Val for Ile substitution at P8 resulted in a 27% reduction in the affinity of CD94-NKG2A for HLA-E, suggesting that the avidity of the interaction between

CD94-NKG2A and HLA-E expressed on normal cells may vary substantially, not only as a function of the amount of HLA-E expressed at the cell surface but in a manner that is dependent on the HLA genotype of the individual.

To provide insight into the footprint CD94-NKG2A adopted on HLA-E and the relative importance of both CD94 and NKG2A in this interaction, we undertook an alanine-scanning approach, assessing the impact of mutations on the affinity of the interaction between CD94-NKG2A and HLA-E. Mutation of Gln72, Arg75, Val76, Glu152, and Asp162 of HLA-E all markedly impaired the affinity of the interaction with CD94-NKG2A, confirming earlier observations by Wada et al. (2004), who showed that mutations at residues 72, 75, and 162 largely abrogated binding of HLA-E tetramers to cells that express CD94-NKG2A.

Mutagenesis of CD94-NKG2A suggested that CD94 played a much more prominent role in the interaction with HLA-E than NKG2A, which was largely attributable to an energetic hotspot that includes residues Gln112, Phe114, Asn160, Leu162, Asp163, and Glu164 of CD94. Accordingly, based on (1) the structural homology between the CD94-NKG2A-HLA-E interaction and that of NKG2D with MIC-A (Li et al., 2001), (2) mutagenesis data on HLA-E (Wada et al., 2004), (3) mutagenesis data on CD94-NKG2A, and (4) the observation that changes in peptide sequence impacted equally on CD94-NKG2A, -C, and -E (Kaiser et al., 2005), evidence suggested that the CD94 subunit was located primarily over the α1 helix of HLA-E making contact with the exposed side chain at P8. The data here provide direct support for a model in which the energetic hotspot bounded by residues 73, 75, 76 of HLA-E together with the side chain of P8 interact with the residues that comprise the energetic hotspot of CD94. Moreover, there appears to be a degree of complementarity between these regions of HLA-E and CD94 that would allow for hydrophobic interactions between residues Val76 of HLA-E together with Phe at P8 of the peptide with Leu112 and Phe114 of CD94. There is also a degree of charge complementarity here as the energetic hotspot on HLA-E is bounded by Arg75 and Arg79, whereas this region of CD94 contains an Asp and Glu at positions 163 and 164, respectively. Our data also provide insight into the basis for the difference in affinity between CD94-NKG2A and CD94-NKG2C for HLA-E, whereby NKG2 residues at the CD94-NKG2 interface appear to determine this affinity differential. Collectively, our data reveals the detailed architecture of the CD94-NKG2A heterodimer and provides insight into the basis of the central innate interaction between this NK heterodimer and the class Ib molecule HLA-E.

EXPERIMENTAL PROCEDURES

Protein Expression and Purification of CD94-NKG2A

The recombinant baculovirus coexpression of CD94 and NKG2A was achieved by cloning residues 34–179 of CD94 and 100–233 of NKG2A into the BamHI and PstI sites and the SphI and XmaI sites of the pFastBac Dual vector, respectively. This allowed incorporation of the CD94 and NKG2A into the bacmid DNA via transposition of pFastBac CD94-NKG2A into DH10Bac *E. coli* (Invitrogen). The sequence of the pFastBac CD94-NKG2A plasmid was verified via sequencing, and the correct incorporation of the CD94-NKG2A cassette into the bacmid DNA was verified via PCR. The viral titer of the resulting bacmid was then amplified in Sf9 insect cells (Invitrogen) grown at 27°C with shaking at 120 rpm, and the virus located in the supernatant was separated from the insect cells via centrifugation at 500 × g in an Eppendorf benchtop centrifuge. The expression of CD94-NKG2A was achieved typically in 4× 1 L flasks of Hi-5 insect cells at 2.0 × 10^6 cells/ml (Invitrogen) by infection with the amplified viral stocks for approximately 68–72 hr at 27°C with shaking at 120 rpm. All Sf9 and Hi5 insect cells were grown at 27°C in GIBCO SF900 II serum-free media (Invitrogen) in the presence of 10 mg/ml Gentamycin.

The CD94-NKG2A protein was secreted into the media by the Hi5 cells, and separation of the secreted protein from whole cells was achieved via centrifugation at 500 × g followed by centrifugation at 5000 × g in a SLC-6000 Beckman rotor for further purification. The supernatant containing CD94-NKG2A was then filtered through a 0.2 μm filter and concentrated to 1 L, and buffer was exchanged into TBS (10 mM Tris-HCl [pH 8.0], 150 mM NaCl) with Tangental flow apparatus (624S model, Waton Marlow). The supernatant was then applied to pre-equilibrated Nickel affinity sepharose (GE Healthcare) and eluted with 300 mM Imidazole in TBS according to manufacturer instructions. The eluted CD94-NKG2A was then further purified on a Superdex 200 16/60 (GE Healthcare) gel filtration column operating on an Akta Purifier system (GE Healthcare) prior to removal of the His_6 affinity tag via Enterokinase (Genscript, USA) at 4°C overnight according to manufacturer's instructions. The cleaved His_6 tag was separated from CD94-NKG2A by passing over Nickel sepharose. The unbound CD94-NKG2A was then further purified on a MonoQ column with a 0%–30% gradient of 1 M NaCl in 10 mM Tris-HCl (pH 8.0). The resulting protein was then quantified against BSA standards and absorbance for further use.

For expression with *E. coli*, the extracellular domains of CD94 and NKG2A (CD94 residues 40–179, NKG2A residues 110–223) were cloned separately into the modified pET-30 expression vector, and the proteins were solubilized from inclusion bodies after expression in *E. coli* as above. Inclusion bodies were mixed 1:2 CD94:NKG2A and also refolded by dilution as described for the KK50.4 TCR (Hoare et al., 2006). CD94-NKG2A complexes were purified by anion exchange and gel filtration chromatography, prior to an additional purification step by MonoQ.

Crystallization, Data Collection, Structure Determination, and Refinement

Crystals of CD94-NKG2A heterodimer were grown in 1.0–1.4 M trisodium citrate, 0.1 M HEPES (pH 6.7–7.3). The crystals were flash frozen at 100°K with 15% glycerol as a cryoprotectant. A 2.5 Å data set was collected at the IMCA beamline (Advanced Photon Source, Chicago) with a *Quantum 210 CCD*. The data were processed and scaled with programs from the CCP4 suite (CCP4, 1994). The crystal structure of the heterodimer was solved by molecular replacement implemented by Phaser (McCoy et al., 2005) with CD94 as the search model. For NKG2A, all differences in the search model were mutated to alanine, and surface loops were removed. The progress of refinement was monitored by the R_{free} value (5% of the data) with neither a σ nor a low-resolution cut-off being applied to the data. The structure was refined with Refmac (CCP4, 1994) and simulated annealing implemented in CNS (Brünger et al., 1998), interspersed with rounds of model building in "Coot" (Emsley and Cowtan, 2004). For the data collection and refinement statistics, see Table 1.

Mutagenesis and Surface Plasmon Resonance Measurements

Production of Soluble, Recombinant Proteins

cDNA encoding the extracellular domain of wild-type HLA-E*0103 and human β_2-microglobulin (β_2m) were cloned into a modified pET-30 expression vector (Boyington et al., 2000). After expression in the *E. coli*

strain BL21 (DE3) pLysS, the proteins were solubilized from inclusion bodies and refolded with synthetic peptides (GL Biochem, Shanghai, China) as previously described (Hoare et al., 2006). The resulting HLA-E-peptide complexes were purified by anion exchange and gel filtration chromatography. Site-directed mutations were generated by the QuikChange Site-Directed Mutagenesis Kit (Stratagene, La Jolla, CA), and the sequence of the mutated cDNA was verified by DNA sequencing. The residues chosen for mutagenesis were surface exposed residues and thus were considered unlikely to affect stability of either the HLA-E complex or the CD94-NKG2A receptor. All of the mutants eluted with a similar gel filtration profile to the wild-type protein. Mutant HLA-E molecules were also assessed for their ability to bind to both a pan-anti-HLA class I specific mAb (w6/32) and anti-human β2-microglobulin by capture ELISA. At the same concentrations, all mutants gave a similar OD reading to wild-type HLA-E. The conformational integrity of mutant CD94-NKG2A receptors was verified by ELISA with conformationally sensitive mAb specific for either CD94 or NKG2A.

BIAcore Analysis

The interaction between soluble, recombinant HLA-E and CD94-NKG2A was analyzed by surface plasmon resonance (SPR) with a BIAcore 3000 instrument (BIAcore, Piscataway, NJ). All experiments were performed at 25°C in a buffer containing 10 mM HEPES (pH 7.4), 150 mM NaCl, and 0.005% Surfactant P-20 (BIAcore). CD94-NKG2A was diluted into 10 mM sodium acetate (pH 5.5), and ~500 RU was immobilized a CM5 Sensorchip (BIAcore) by amine coupling as recommended by the manufacturer. Each chip contained two different preparations of immobilized CD94-NKG2A and two control surfaces. Recombinant HLA-E was subjected to size exclusion chromatography immediately prior to analysis, and the concentration of purified protein was estimated with a Bradford assay. It was then serially diluted from 20 μM to 0.05 μM in HBS and injected simultaneously over the test and control surfaces at a flow rate of 40 μL/min. All measurements were taken in duplicate and results from at least two independent experiments were analyzed. After subtraction of data from control flow cells, the interactions were analyzed with the BIAevaluation software version 4.1 (BIAcore) and steady-state K_D values were derived from the general fit option of the software package.

Supplemental Data

Two figures and two tables are available at http://www.immunity.com/cgi/content/full/27/6/900/DC1/.

ACKNOWLEDGMENTS

We would like to thank the staff at IMCA, Advanced Photon Source, Chicago, IL, for assistance with data collection. This work was supported by grants from the NHMRC, the Australian Research Council (ARC), an ARC Federation Fellowship (J.R.), an ARC QEII fellowship (C.S.C.), and Peter Doherty Fellowships from the NHMRC (L.C.S. and T.B.).

Received: June 22, 2007
Revised: September 27, 2007
Accepted: October 25, 2007
Published online: December 13, 2007

REFERENCES

Bellón, T., Heredia, A.B., Llano, M., Minguela, A., Rodriguez, A., López-Botet, M., and Aparicio, P. (1999). Triggering of effector functions on a $CD8^+$ T cell clone upon the aggregation of an activatory CD94/kp39 heterodimer. J. Immunol. *162*, 3996–4002.

Bland, F.A., Lemberg, M.K., McMichael, A.J., Martoglio, B., and Braud, V.M. (2003). Requirement of the proteasome for the trimming of signal peptide-derived epitopes presented by the nonclassical major histocompatibility complex class I molecule HLA-E. J. Biol. Chem. *278*, 33747–33752.

Borrego, F., Ulbrecht, M., Weiss, E.H., Coligan, J.E., and Brooks, A.G. (1998). Recognition of human histocompatibility leukocyte antigen (HLA)-E complexed with HLA class I signal sequence-derived peptides by CD94/NKG2 confers protection from natural killer cell-mediated lysis. J. Exp. Med. *187*, 813–818.

Borrego, F., Masilamani, M., Marusina, A.I., Tang, X., and Coligan, J.E. (2006). The CD94/NKG2 family of receptors: from molecules and cells to clinical relevance. Immunol. Res. *35*, 263–278.

Boyington, J.C., Riaz, A.N., Patamawenu, A., Coligan, J.E., Brooks, A.G., and Sun, P.D. (1999). Structure of CD94 reveals a novel C-type lectin fold: implications for the NK cell-associated CD94/NKG2 receptors. Immunity *10*, 75–82.

Boyington, J.C., Motyka, S.A., Schuck, P., Brooks, A.G., and Sun, P.D. (2000). Crystal structure of an NK cell immunoglobulin-like receptor in complex with its class I MHC ligand. Nature *405*, 537–543.

Braud, V.M., Allan, D.S., O'Callaghan, C.A., Soderstrom, K., D'Andrea, A., Ogg, G.S., Lazetic, S., Young, N.T., Bell, J.I., Phillips, J.H., et al. (1998a). HLA-E binds to natural killer cell receptors CD94/NKG2A, B and C. Nature *391*, 795–799.

Braud, V.M., Allan, D.S., Wilson, D., and McMichael, A.J. (1998b). TAP- and tapasin-dependent HLA-E surface expression correlates with the binding of an MHC class I leader peptide. Curr. Biol. *8*, 1–10.

Brooks, A.G., Posch, P.E., Scorzelli, C.J., Borrego, F., and Coligan, J.E. (1997). NKG2A complexed with CD94 defines a novel inhibitory natural killer cell receptor. J. Exp. Med. *185*, 795–800.

Brooks, A.G., Borrego, F., Posch, P.E., Patamawenu, A., Scorzelli, C.J., Ulbrecht, M., Weiss, E.H., and Coligan, J.E. (1999). Specific recognition of HLA-E, but not classical, HLA class I molecules by soluble CD94/NKG2A and NK cells. J. Immunol. *162*, 305–313.

Brostjan, C., Bellon, T., Sobanov, Y., Lopez-Botet, M., and Hofer, E. (2002). Differential expression of inhibitory and activating CD94/NKG2 receptors on NK cell clones. J. Immunol. Methods *264*, 109–119.

Brünger, A.T., Adams, P.D., Clore, G.M., DeLano, W.L., Gros, P., Grosse-Kunstleve, R.W., Jiang, J.S., Kuszewski, J., Nilges, M., Pannu, N.S., et al. (1998). Crystallography and NMR system: a new software suite for macromolecular structure determination. Acta Crystallogr. D Biol. Crystallogr. *54*, 905–921.

Carretero, M., Cantoni, C., Bellon, T., Bottino, C., Biassoni, R., Rodriguez, A., Perez-Villar, J.J., Moretta, L., Moretta, A., and Lopez-Botet, M. (1997). The CD94 and NKG2-A C-type lectins covalently assemble to form a natural killer cell inhibitory receptor for HLA class I molecules. Eur. J. Immunol. *27*, 563–567.

Cella, M., Nakajima, H., Facchetti, F., Hoffmann, T., and Colonna, M. (2000). ILT receptors at the interface between lymphoid and myeloid cells. Curr. Top. Microbiol. Immunol. *251*, 161–166.

Collaborative Computational Project, Number 4 (1994). The CCP4 suite: programs for protein crystallography. Acta Crystallogr. D Biol. Crystallogr. *50*, 760–763.

Emsley, P., and Cowtan, K. (2004). Coot: model-building tools for molecular graphics. Acta Crystallogr. D Biol. Crystallogr. *60*, 2126–2132.

Hoare, H.L., Sullivan, L.C., Pietra, G., Clements, C.S., Lee, E.J., Ely, L.K., Beddoe, T., Falco, M., Kjer-Nielsen, L., Reid, H.H., et al. (2006). Structural basis for a major histocompatibility complex class Ib-restricted T cell response. Nat. Immunol. *7*, 256–264.

Houchins, J.P., Yabe, T., McSherry, C., and Bach, F.H. (1991). DNA sequence analysis of NKG2, a family of related cDNA clones encoding type II integral membrane proteins on human natural killer cells. J. Exp. Med. *173*, 1017–1020.

Houchins, J.P., Lanier, L.L., Niemi, E.C., Phillips, J.H., and Ryan, J.C. (1997). Natural killer cell cytolytic activity is inhibited by NKG2-A and activated by NKG2-C. J. Immunol. *158*, 3603–3609.

Kaiser, B.K., Barahmand-Pour, F., Paulsene, W., Medley, S., Geraghty, D.E., and Strong, R.K. (2005). Interactions between

NKG2x immunoreceptors and HLA-E ligands display overlapping affinities and thermodynamics. J. Immunol. *174*, 2878–2884.

Kim, D.K., Kabat, J., Borrego, F., Sanni, T.B., You, C.H., and Coligan, J.E. (2004). Human NKG2F is expressed and can associate with DAP12. Mol. Immunol. *41*, 53–62.

Kogelberg, H., and Feizi, T. (2001). New structural insights into lectin-type proteins of the immune system. Curr. Opin. Struct. Biol. *11*, 635–643.

Lanier, L.L., Corliss, B., Wu, J., and Phillips, J.H. (1998). Association of DAP12 with activating CD94/NKG2C NK cell receptors. Immunity *8*, 693–701.

Lazetic, S., Chang, C., Houchins, J.P., Lanier, L.L., and Phillips, J.H. (1996). Human natural killer cell receptors involved in MHC class I recognition are disulfide-linked heterodimers of CD94 and NKG2 subunits. J. Immunol. *157*, 4741–4745.

Lee, N., Llano, M., Carretero, M., Ishitani, A., Navarro, F., Lopez-Botet, M., and Geraghty, D.E. (1998). HLA-E is a major ligand for the natural killer inhibitory receptor CD94/NKG2A. Proc. Natl. Acad. Sci. USA *95*, 5199–5204.

Li, P., Morris, D.L., Willcox, B.E., Steinle, A., Spies, T., and Strong, R.K. (2001). Complex structure of the activating immunoreceptor NKG2D and its MHC class I-like ligand MICA. Nat. Immunol. *2*, 443–451.

Li, P., McDermott, G., and Strong, R.K. (2002). Crystal structures of RAE-1beta and its complex with the activating immunoreceptor NKG2D. Immunity *16*, 77–86.

Lieto, L.D., Maasho, K., West, D., Borrego, F., and Coligan, J.E. (2006). The human CD94 gene encodes multiple, expressible transcripts including a new partner of NKG2A/B. Genes Immun. *7*, 36–43.

Llano, M., Lee, N., Navarro, F., Garcia, P., Albar, J.P., Geraghty, D.E., and Lopez-Botet, M. (1998). HLA-E-bound peptides influence recognition by inhibitory and triggering CD94/NKG2 receptors: preferential response to an HLA-G-derived nonamer. Eur. J. Immunol. *28*, 2854–2863.

Lodoen, M.B., and Lanier, L.L. (2005). Viral modulation of NK cell immunity. Nat. Rev. Microbiol. *3*, 59–69.

McCoy, A.J., Storoni, L.C., Grosse-Kunstleve, R.W., and Read, R.J. (2005). Likelihood-enhanced fast translation functions. Acta Crystallogr. D Biol. Crystallogr. *61*, 458–464.

McFarland, B.J., and Strong, R.K. (2003). Thermodynamic analysis of degenerate recognition by the NKG2D immunoreceptor: not induced fit but rigid adaptation. Immunity *19*, 803–812.

McFarland, B.J., Kortemme, T., Yu, S.F., Baker, D., and Strong, R.K. (2003). Symmetry recognizing asymmetry: analysis of the interactions between the C-type lectin-like immunoreceptor NKG2D and MHC class I-like ligands. Structure *11*, 411–422.

Miller, J.D., Weber, D.A., Ibegbu, C., Pohl, J., Altman, J.D., and Jensen, P.E. (2003). Analysis of HLA-E peptide-binding specificity and contact residues in bound peptide required for recognition by CD94/NKG2. J. Immunol. *171*, 1369–1375.

Natarajan, K., Sawicki, M.W., Margulies, D.H., and Mariuzza, R.A. (2000). Crystal structure of human CD69: a C-type lectin-like activation marker of hematopoietic cells. Biochemistry *39*, 14779–14786.

Sawicki, M.W., Dimasi, N., Natarajan, K., Wang, J., Margulies, D.H., and Mariuzza, R.A. (2001). Structural basis of MHC class I recognition by natural killer cell receptors. Immunol. Rev. *181*, 52–65.

Tormo, J., Natarajan, K., Margulies, D.H., and Mariuzza, R.A. (1999). Crystal structure of a lectin-like natural killer cell receptor bound to its MHC class I ligand. Nature *402*, 623–631.

Vales-Gomez, M., Reyburn, H.T., Erskine, R.A., Lopez-Botet, M., and Strominger, J.L. (1999). Kinetics and peptide dependency of the binding of the inhibitory NK receptor CD94/NKG2-A and the activating receptor CD94/NKG2-C to HLA-E. EMBO J. *18*, 4250–4260.

Vance, R.E., Kraft, J.R., Altman, J.D., Jensen, P.E., and Raulet, D.H. (1998). Mouse CD94/NKG2A is a natural killer cell receptor for the nonclassical major histocompatibility complex (MHC) class I molecule Qa-1(b). J. Exp. Med. *188*, 1841–1848.

Vance, R.E., Jamieson, A.M., and Raulet, D.H. (1999). Recognition of the class Ib molecule Qa-1(b) by putative activating receptors CD94/NKG2C and CD94/NKG2E on mouse natural killer cells. J. Exp. Med. *190*, 1801–1812.

Wada, H., Matsumoto, N., Maenaka, K., Suzuki, K., and Yamamoto, K. (2004). The inhibitory NK cell receptor CD94/NKG2A and the activating receptor CD94/NKG2C bind the top of HLA-E through mostly shared but partly distinct sets of HLA-E residues. Eur. J. Immunol. *34*, 81–90.

Wolan, D.W., Teyton, L., Rudolph, M.G., Villmow, B., Bauer, S., Busch, D.H., and Wilson, I.A. (2001). Crystal structure of the murine NK cell-activating receptor NKG2D at 1.95 A. Nat. Immunol. *2*, 248–254.

Wu, J., Song, Y., Bakker, A.B., Bauer, S., Spies, T., Lanier, L.L., and Phillips, J.H. (1999). An activating immunoreceptor complex formed by NKG2D and DAP10. Science *285*, 730–732.

Accession Numbers

Coordinates have been deposited in Protein Data Bank with accession code 3BDW.